Journal of
Nanoscience and Nanotechnology
Vol. 9, 1412–1417, 2009

RESEARCH ARTICLE

# Epoxy Resin Filled with High Volume Content Nano-$SiO_2$ Particles

Sheng Liu[1], Hui Zhang[1], Zhong Zhang[1,*], and Stephan Sprenger[2]

[1] National Center for Nanoscience and Technology, China, 100080 Beijing, China
[2] Nanoresins AG, 21502 Geesthacht, Germany

Mechanical and thermal properties of $SiO_2$/epoxy nanocomposites with almost uniformly dispersed nanoparticles were thoroughly investigated in this study. Young's modulus, tensile strength and fracture toughness of epoxy resin were simultaneously improved with $SiO_2$ nanoparticles up to 14 vol.%. Atomic force microscopy was carried out in order to detect the nanoparticle-matrix interphase. It was found that the interphase region became harder than the bulk matrix, due to the higher crosslink density in the interphase region. Differential scanning calorimetry was applied to investigate the curing behaviors of nano-$SiO_2$/epoxy composites. The presence of nano-$SiO_2$ had little effects on the curing reaction. In addition, the glass transition temperature of epoxy resin dropped slightly with the increased nano-$SiO_2$ content.

**Keywords:** Nanocomposites, Epoxy, Atomic Force Microscopy, Interphase.

## 1. INTRODUCTION

Epoxy resins have been widely used in various industrial applications, particularly for wear resistant coatings, adhesives and matrices of advanced fiber reinforced composites.[1–3] In spite of their excellent performance, such as good mechanical behavior, excellent solvent resistance and high electrical resistance, highly-cured epoxy resins often exhibit undesirably brittle nature due to their highly cross-linked network. Epoxy resins are very sensitive to cracks and local stress concentrations, which may lead to brittle failure.[4] In order to improve the fracture toughness, intensive attempts have been developed of multiphase composites filled with various additives, such as rubbers,[5] thermoplastics[6,7] and inorganic particles.[8] In the last decade various nano-fillers have been applied to improve the mechanical properties of epoxy resin.[9,10] This is because that the nano-fillers have large interphase region, which could play an essential role in the mechanical properties of epoxy. However, an inherent problem in manufacturing nanocomposites is the agglomeration of nano-fillers. Big agglomerations usually act as the defects promoting a premature failure and in turn destroying the mechanical properties of the composite materials.

In this work, $SiO_2$/epoxy nanocomposites with almost homogeneously dispersed nanoparticles were produced by a special sol–gel technique. Mechanical properties of nanocomposites as a function of nano-$SiO_2$ volume content were studied in terms of tensile properties and fracture toughness. The nanoparticle-matrix interphase and curing behaviors of uncured systems were studied also.

## 2. EXPERIMENTAL DETAILS

### 2.1. Materials

The $SiO_2$/epoxy master batch prepared via a special sol–gel technique was supplied by nanoresins AG, Germany (Nanopox E470). It contains ~40 wt% of spherical $SiO_2$ nanoparticles and ~60 wt% neat bisphenol-A epoxy resin. The methylhexahydrophthalic anhydride (MHHPA) was chosen to serve as the hardener. The master batch was mechanically mixed with given amounts of neat epoxy resin to prepare a series of nanocomposites with desired $SiO_2$ contents. Then the stoichiometric amounts of hardener were added to the mixtures and further stirred for 30 min at 60 °C. After degassing under vacuum, the mixtures were cast into preheated steel moulds and cured at 120 °C for 1 h, followed by a post-cure at 160 °C for 2 h. The final nanocomposites contained 1, 3, 6, 9, 14 vol.% $SiO_2$ contents, respectively. In this work they were referred to as A1, A3, A6, A9 and A14, respectively.

### 2.2. Characterizations

#### *2.2.1. TEM and SEM*

Thin sections, 60–90 nm in thickness, were cut from bulk composites using an ultramicrotome (LKB Nova)

*Author to whom correspondence should be addressed.



1533-4880/2009/9/1412/006 doi:10.1166/jnn.2009.C168

equipped with a diamond knife. The sections were observed by transmission electron microscopy (FEI Tecnai20) at an accelerating voltage of 120 kV. The fracture surfaces taken from tensile samples were examined by scanning electron microcopy (HITAHI S-4300) after gold sputtering.

#### 2.2.2. AFM

The interphase between nano-$SiO_2$ particles and epoxy matrix was detected using atomic force microscopy (AFM, Nanoscope IIIa, Digital Instruments. Co.). A tapping mode was used in this work. The X-Y and Z motions of the cantilever were controlled using a calibrated piezoelectric tube incorporated into the AFM head. Topography and phase images were acquired using $512 \times 512$ pixels and a scan rate of 1 Hz in the tapping mode of operation.

#### 2.2.3. Mechanical Properties

The tensile tests were conducted using an Instron 5848 micro-Tester according to ASTM D-638. The crosshead speed was kept constant at 1 mm/min. Quasi-static fracture toughness tests were carried out using compact tension (CT) specimens with dimensions of $36 \times 36 \times 7.5$ $mm^3$. A pre-crack was made by lightly tapping a sharp fresh razor blade into the bottom of the saw slot in the specimen. With this method, the crack can pop into the material over several millimeters, thus yielding a natural crack. The tensile loading of the CT specimens was accomplished on an Instron 5848 micro-Tester at a crosshead speed of 1 mm/min. The actual crack length was measured after the fracture test by an optical microscope equipped with a micrometer scale. At least five specimens were tested for each composite.

#### 2.2.4. Curing Kinetics and Thermal Properties

The curing kinetics of uncured mixtures of $SiO_2$/epoxy/MHHPA was performed on differential scanning calorimeter (Pyris Diamond DSC). The mixture of 10–20 mg was degassed in vacuum first, and then it was sealed in hermetic pans and heated from room temperature to 350 °C under $N_2$ atmosphere. The heating rates were 2, 5, 10, and 15 °C/min, respectively. The curing kinetic parameters of the blends were examined by Kissinger's approach.[11–13] The relationship between apparent activation energy $\Delta E$ (J/mol), the constant heating rate $\beta$ (K/min) and the temperature $T_p$ (K) at which the exothermic peak has its maximum can be described as:

$$\ln\left(\frac{\beta}{T_p^2}\right) = \ln\left(\frac{RA}{\Delta E}\right) - \frac{\Delta E}{R}\frac{1}{T_p} \quad (1)$$

where $R$ is the gas constant, equal to 8.314 J/mol · K, $A$ is the pre-exponential factor. From the non-isothermal DSC curves measured at different heating rates, the linear relation between $\ln(\beta/T_p^2)$ and $1/T_p$ can be obtained. Therefore, the values of $\Delta E$ and $\ln A$ can be calculated, respectively, from the slope and intercept of linear regression of Eq. (1).

The value of $\Delta E$ was introduced to the Crane equation,[14] which is expressed as:

$$\frac{d(\ln\beta)}{d(1/T_p)} \approx -\frac{\Delta E}{nR} \quad (2)$$

then the reaction order $n$ can be calculated by the slope coefficient of $\ln\beta$ versus $1/T_p$.

## 3. RESULTS AND DISCUSSION

### 3.1. Dispersion of $SiO_2$ Nanoparticles in Epoxy Matrix

TEM is a straightforward way to visualize the dispersion quality of nanoparticles within polymer matrix. Figure 1 shows the images of $SiO_2$ nanoparticles in epoxy matrix with the content of 1, 9 and 14 vol.%. It can be found that $SiO_2$ nanoparticles are spheres with average size of 20 nm. Obviously, an agglomerate-free state of $SiO_2$ nanoparticles in epoxy matrix is reached even at high volume content, which is a prerequisite for improvements of mechanical properties of $SiO_2$/epoxy nanocomposites.

### 3.2. Interphase Characterizations

It has been widely accepted that the interphase between filler and matrix plays a key role in the properties of polymer composites, since stress concentration often occurs at the interphase regions, depending on the geometry of the particles and the differences of the thermal expansion. It has been reported that the thickness of the interphase in nanocomposites ranged from a few nanometers to a fraction of micrometer.[15, 16] Although the importance of the interphase has been accepted, up to now experimental visualization of the interphase between nano-fillers and matrix is not yet fully available.

Recently, the development of atomic force microscopy (AFM) methods has provided a new capability for determining polymer morphology with nanometer and better spatial resolution.[17] In tapping mode, height and phase images are simultaneously monitored. For height images, the higher domains in the surface of specimens appear brighter and the lower ones appear darker. Comparatively, for the phase maps, the higher modulus (stiffer) domains appear lighter and the lower ones (softer) appear darker. Although absolute value of modulus can not be determined by the AFM used in this study, it can still be used to identify matrix and inorganic phases and to follow the modulus differences in the surface of specimens caused by cross-linking density changes.

Figure 2 shows the height image, phase image and surface cross-sectional profile, measured from an identical

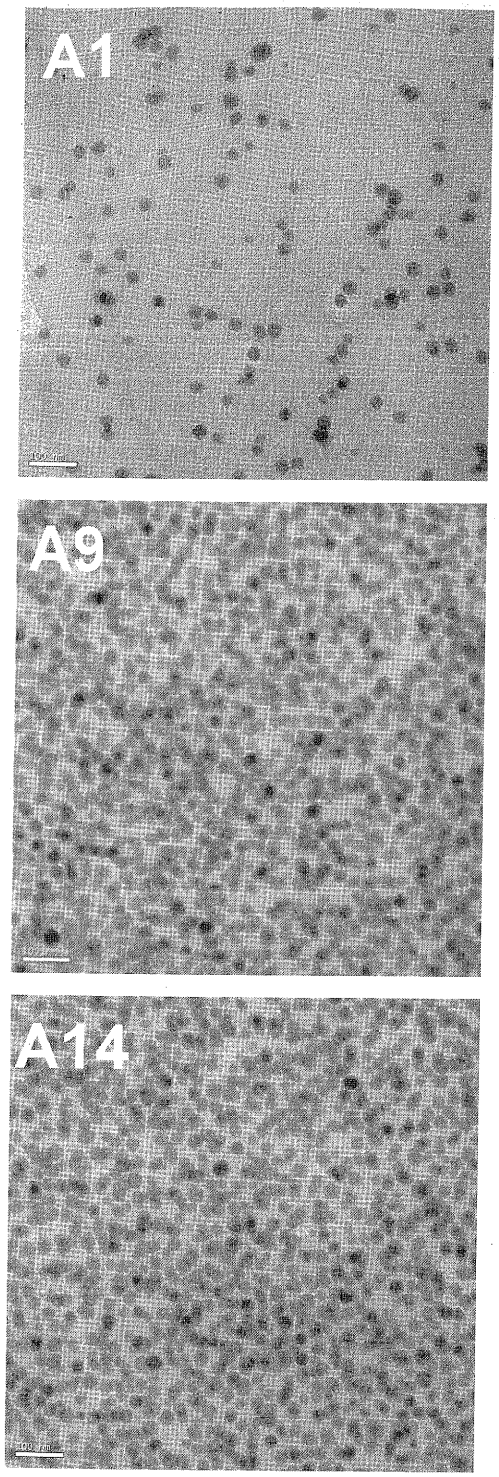


**Fig. 1.** TEM images of $SiO_2$/epoxy nanocomposites with different nanoparticles content.

area of the nanocomposite containing 3 vol.% $SiO_2$. In the height image, the brighter parts marked by arrows "a" should be the primary nanoparticles, because they protuberate on the surface and have round shape. Moreover, the cross-section profile indicates that their size is around 37 nm. This value approximates the average diameter of nanoparticles (20 nm) measured by TEM. Likewise, the darker parts marked by arrows "b" should be the voids after nanoparticle debonding and fallout.

An interesting phenomenon can be observed in the phase image: All the primary nanoparticles and the voids are brighter. As discussed above, brighter color is related to higher stiffness in the phase image. This means that the void area is stiffer than the bulk matrix material. The background in the phase image represents the bulk matrix material, which is relatively soft and thus appears darker. In other words, the interphase area is stiffer than the bulk matrix material. Olmos et al.[18] reported that the silica particles could absorb excessive hardener around them and thus changing the homogeneity of epoxy network. The phenomenon observed in the present work could be also explained by this point, i.e., due to the physicochemical interaction, the anhydride hardener can be enriched in the vicinity of nanoparticles, which increases the local cross-linking density and the related stiffness of the interphase.

### 3.3. Mechanical Properties and Morphologies

#### *3.3.1. Tensile Properties*

Mechanical tests were performed to quantify the overall effect of the filler on the performance of composites. Young's modulus ($E$) and tensile strength ($\sigma_b$) as a function of nano-$SiO_2$ volume fraction are given in Figure 3. The Young's modulus of nanocomposites almost linearly increases with nano-$SiO_2$ particle content. The Young's modulus of 3.95 GPa measured for 14 vol.% nano-$SiO_2$/epoxy is enhanced by about 44% as compared to 2.75 GPa of neat epoxy. This is easily understood because the modulus of $SiO_2$ (70 GPa[19]) is much higher than that of the neat epoxy. The linear increase of Young's modulus of epoxy resin with increasing of nano-$SiO_2$ content is well fitted with Halpin-Tsai model.[19] Since this model describes perfect bonding between filler and matrix, it is reasonable to consider that the similar case should occur in our nanocomposites. This means that strong adhesion was formed between nano-$SiO_2$ particles and epoxy resin. As known, strong adhesion promotes stress transfer between two phases in composites.

#### *3.3.2. Fracture Toughness and Morphologies*

Figure 4 shows the results of fracture toughness ($K_{IC}$). The $K_{IC}$ measured by a compact tension approach was significantly improved by the addition of $SiO_2$ nanoparticles. An average value $K_{IC}$ improved from 0.546 MPa $\cdot$ $m^{1/2}$ of unmodified epoxy to a maximum of 0.833 MPa $\cdot$ $m^{1/2}$ of nanocomposites with 14 vol.% nano-$SiO_2$, which has been enhanced by more than 50%.

SEM micrographs of fracture surface of tensile specimens with different $SiO_2$ content are shown in Figure 5.

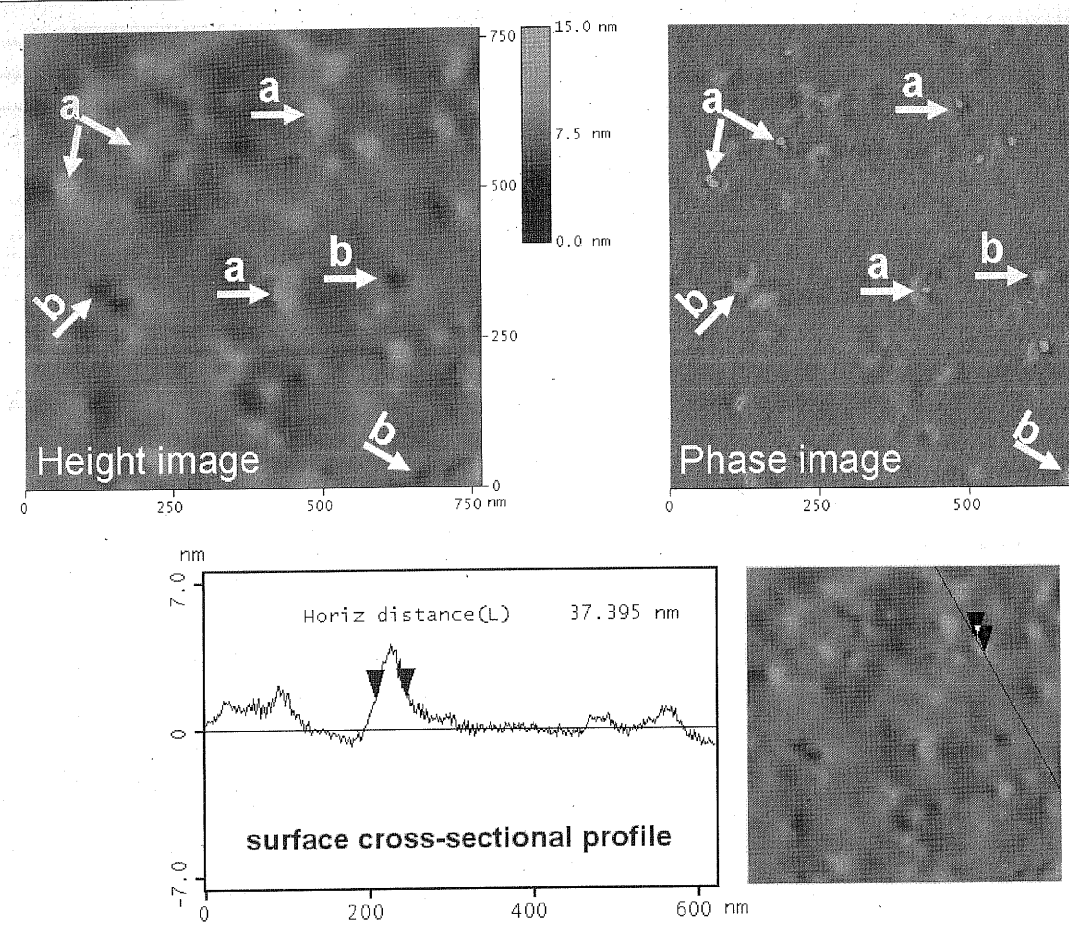


**Fig. 2.** AFM images of height, phase and surface cross-sectional profile of epoxy with 3 vol.% nano-$SiO_2$.

Different fracture surfaces can be seen between the neat epoxy and nanocomposites, which indicate the different fracture mechanisms. In the neat epoxy the fracture surface is relatively smooth. However, rougher fracture surface and a lot of dimples with irregular shapes can be observed in the nanocomposites. The number of dimples increases with the nano-fillers content, which would consume more energy during fracture.

For rigid micron-sized particle/epoxy systems, the related toughening mechanisms[20, 21] have frequently been shown to be due to: (1) an increase in fracture surface

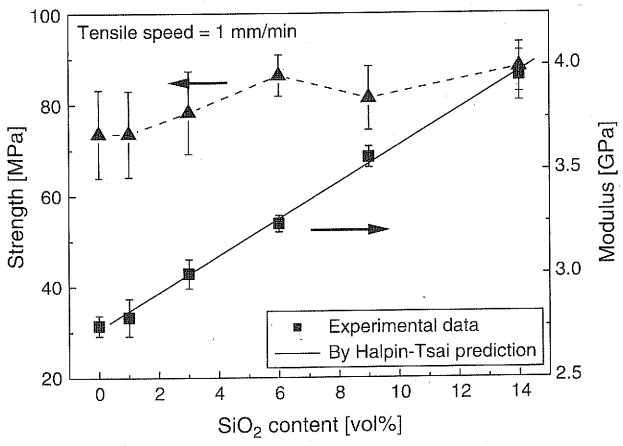


**Fig. 3.** Tensile strength and modulus of epoxy resin as a function of nano-$SiO_2$ volume fraction.

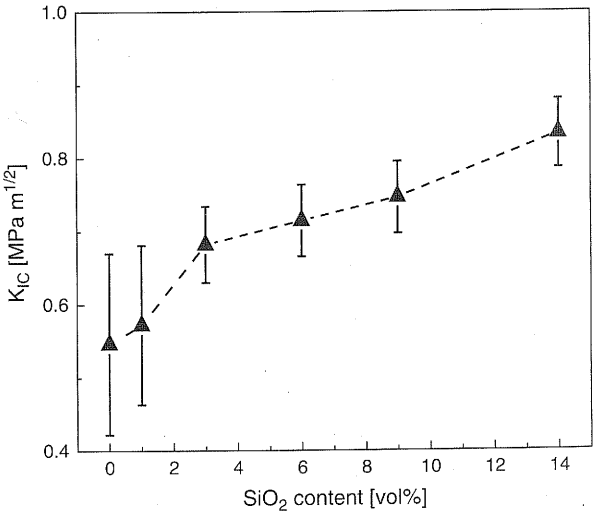


**Fig. 4.** Fracture toughness of epoxy resin as a function of nano-$SiO_2$ volume fraction.

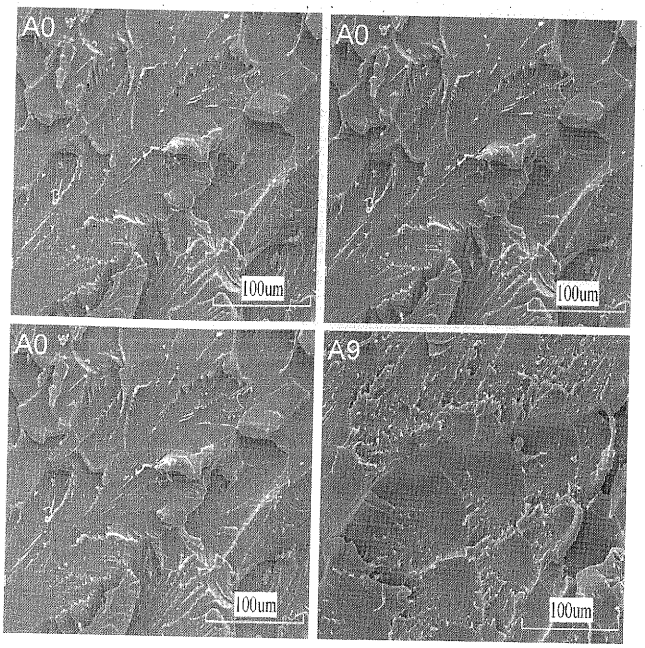


**Fig. 5.** SEM micrographs of fracture surfaces taken from tensile tests.

area caused by crack deflection and crack twisting around particles; (2) crack-front pinning effect of rigid particles; (3) enhanced plastic deformation of the epoxy around the particles. Generally, these toughening mechanisms do not take into account the contributions of particle-matrix interphase and would not be suitable for the nanoparticle-toughening system.

Considering the size effect of nanoparticles,[22] other toughening mechanism was suggested. When the distance between nanoparticles reduced to smaller than a critical interparticle distance nanoparticles could enhance the toughening effect. This would be due to the fact that nanofillers can influence the epoxy network structure, especially the near surface zone during curing process. And this was affirmed by results from Rosso et al.[23] and our current AFM observations, where a polymer shell was directly observed around the rigid nanoparticle. Zhang et al.[24] investigated the correlations between interparticle distance and mechanical properties and further pointed out that when the nanoparticle volume content was up to 7%, the distance between nanoparticles would be smaller than the diameter of nanoparticles. Therefore the interphase surround the nanoparticles may structure a 3D network in the matrix, and finally dominate the performance of the nanocomposites. Nevertheless further work is still needed for developing and understanding the toughening mechanism of nanoparticles.

### 3.4. Curing Reaction Kinetics Analysis and Thermal Properties

Figure 6 shows non-isothermal DSC curves for DGEBA/MHHPA and DGEBA/MHHPA/9 vol.% nano-$SiO_2$ systems at different heating rates (2, 5, 10, 15 °C/min). The reaction kinetic parameters $\Delta E$, $\ln A$ and $n$ are listed in Table I for all specimens studied. The results show that nano-$SiO_2$ content has little effect on the kinetic parameters values of $SiO_2$/epoxy nanocomposites, which indicates that highly dispersed $SiO_2$ nanoparticles in epoxy resin might not change the nature of curing reaction, even at high nano-$SiO_2$ content. This might be a result of two competitive factors. On the one hand, the hydroxyl groups absorbed onto the surfaces of $SiO_2$

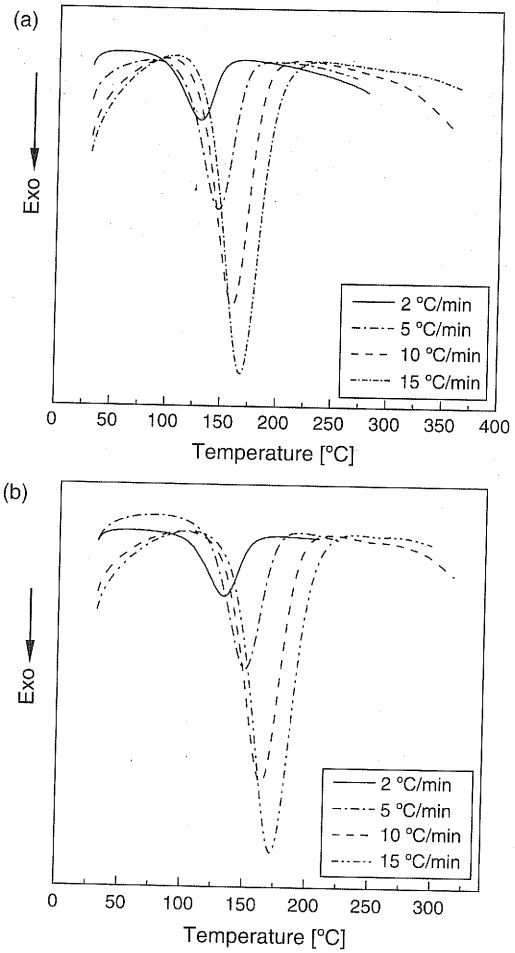


**Fig. 6.** Non-isothermal DSC curves of neat epoxy/MHHPA and 9 vol.% nano-$SiO_2$/epoxy/MHHPA measured at different heating rates.

**Table I.** The curing kinetic parameters of $SiO_2$/epoxy nanocomposites with different nano-$SiO_2$ contents.

| $SiO_2$ content [vol.%] | $\Delta E$ (kJ/mol) | $\ln A$ | $n$ | $T_g$ [°C] |
|---|---|---|---|---|
| 0 | 68.2 | 11.22 | 0.91 | 144.1 |
| 1 | 68.7 | 11.32 | 0.91 | 140.7 |
| 3 | 66.4 | 10.57 | 0.90 | 137.8 |
| 6 | 69.9 | 11.62 | 0.91 | 138.1 |
| 9 | 67.3 | 10.76 | 0.91 | 135.6 |
| 14 | 64.9 | 9.97 | 0.90 | 132.0 |

nanoparticles could act as catalyst in reaction between epoxy and curing agent,[13] which help to lower active energies during the curing reaction. On the other hand, the addition of $SiO_2$ nanoparticles will increase the viscosity of the uncured mixtures, and constrains the mobility of polymer chain, which leads to the active energies increase during the curing reaction. These two competitive factors are offset by each other and then the active energies of nano-$SiO_2$/epoxy systems will remain constant.

The glass transition temperature of $SiO_2$/epoxy nanocomposites is also shown in Table I. It can be found that $T_g$s of $SiO_2$/epoxy nanocomposites decrease with the addition of nano-$SiO_2$, which is in good agreement with the general trend observed in previous work.[25, 26]

## 4. CONCLUSIONS

In the current research, mechanical and thermal properties of epoxy matrix with uniformly dispersed $SiO_2$ nanoparticles were studied. The interphase between nano-$SiO_2$ and epoxy matrix, curing kinetics of nano-$SiO_2$/epoxy systems and morphologies of fracture surfaces were investigated via various approaches in order to understand the microstructure/property relationships. Young's modulus, tensile strength and fracture toughness were improved simultaneously by uniformly dispersed $SiO_2$ nanoparticles even at high volume content. AFM images indicated obvious interphase hardening occurred around nanoparticles, which is likely due to the higher crosslink density herein.

**Acknowledgments:** This work was partly sponsored by a Key Research Program of the Ministry of Science and Technology of China (Grant No. 2006CB932304). The authors are grateful to nanoresins AG for the support of nano-$SiO_2$/epoxy master batch. Acknowledgement is due to Dr. Y.-L. Yang for her assistance on AFM observations. Zhong Zhang and Sheng Liu appreciate the support of a Project Based Personnel Exchange Programme (PPP) with China Scholarship Council (CSC) and German Academic Exchange Service (DAAD).

## References and Notes

1. L. Chang, Z. Zhang, C. Breidt, and K. Friedrich, *Wear* 258, 141 (**2005**).
2. J. Cho, J. Y. Chen, and I. M. Daniel, *Scr. Mater.* 56, 685 (**2007**).
3. A. B. de Morais, A. B. Pereira, J. P. Teixeira, and N. C. Cavaleiro, *Int. J. Adhes. Adhes.* 27, 679 (**2007**).
4. A. S. Argon and R. E. Cohen, *Polymer* 44, 6013 (**2003**).
5. R. Thomas, S. Durix, C. Sinturel, T. Omonov, S. Goossens, G. Groeninckx, P. Moldenaers, and S. Thomas, *Polymer* 48, 1695 (**2007**).
6. T. Yoon, B. S. Kim, and D. S. Lee, *J. Appl. Polym. Sci.* 66, 2233 (**1997**).
7. M. Larranaga, M. D. Martın, N. Gabilondo, G. Kortaberria, M. A. Corcuera, C. C. Riccardi, and I. Mondragon, *Polym. Int.* 53, 1495 (**2004**).
8. G. Xu, M. Gong, and W. Shi, *Polym. Adv. Technol.* 16, 473 (**2005**).
9. Y. Guo and Y. Li, *Mater. Sci. Eng. A-Struct. Mater. Prop. Microstruct. Process.* 458, 330 (**2007**).
10. F. Hussain, M. Hojjati, M. Okamoto, and R. E. Gorga, *J. Compos. Mater.* 40, 1511 (**2006**).
11. G. Xu, W. Shi, and S. Shen, *J. Polym. Sci. Pt. B-Polym. Phys.* 42, 2649 (**2004**).
12. S. Bao, S. Shen, G. Liang, H. B. Zhai, W. B. Xu, and P. S. He, *J. Appl. Polym. Sci.* 92, 3822 (**2004**).
13. Y. Liu, Z. Du, C. Zhang, C. J. Li, and H. Q. Li, *J. Appl. Polym. Sci.* 103, 2041 (**2007**).
14. W. J. Zhao, Z. G. Zhang, Z. J. Sun, and D. X. Zhang, *Acta Polym. Sin.* 4, 564 (**2006**).
15. S. Gao and E. Mäder, *Compos. Pt. A-Appl. Sci. Manuf.* 33, 559 (**2002**).
16. J. Kim, M. Sham, and J. Wu, *Compos. Pt. A-Appl. Sci. Manuf.* 32, 607 (**2001**).
17. Y. Wang and T. H. Hahn, *Compos. Sci. Technol.* 67, 92 (**2007**).
18. D. Olmos, A. J. Aznar, and J. Gonzalez-Benito, *Polym. Test.* 24, 275 (**2005**).
19. B. B. Johnsen, A. J. Kinloch, R. D. Mohammed, A. C. Taylor, and S. Sprenger, *Polymer* 48, 530 (**2007**).
20. S. Deng, L. Ye, and K. Friedrich, *J. Mater. Sci.* 42, 2766 (**2007**).
21. B. Wetzel, P. Rosso, F. Haupert, and K. Friedrich, *Eng. Fract. Mech.* 73, 2375 (**2006**).
22. Y. Zheng, Y. Zheng, and R. Ning, *Mater. Lett.* 57, 2940 (**2003**).
23. P. Rosso and L. Ye, *Macromol. Rapid Commun.* 28, 121 (**2007**).
24. H. Zhang, Z. Zhang, K. Friedrich, and C. Eger, *Acta Mater.* 54, 1833 (**2006**).
25. A. J. Kinloch, R. D. Mohammed, and A. C. Taylor, *J. Mater. Sci.* 40, 5083 (**2005**).
26. P. Rosso, L. Ye, K. Friedrich, and S. Sprenger, *J. Appl. Polym. Sci.* 100, 1849 (**2006**).

Received: 7 June 2007. Accepted: 30 November 2007.